Journal of Photochemistry and Photobiology A: Chemistry 198 (2008) 85–91

Contents lists available at ScienceDirect

Journal of Photochemistry and Photobiology A: Chemistry

journal homepage: www.elsevier.com/locate/jphotochem

Spectroscopic and electrochemical properties of 2-aminophenothiazine

Luis Piñero[a], Xiomara Calderón[a], Juan Rodríguez[a], Ileana Nieves[a], Rafael Arce[b], Carmelo García[a,*], Rolando Oyola[a,*]

[a] University of Puerto Rico at Humacao, Department of Chemistry, Humacao, 100 Road 908, Humacao, PR 00791-4300, United States
[b] University of Puerto Rico at Río Piedras, Department of Chemistry, San Juan, PR 00936, United States

ARTICLE INFO

Article history:
Received 25 January 2008
Received in revised form 20 February 2008
Accepted 25 February 2008
Available online 8 March 2008

Keywords:
Phenothiazine
Tricyclic antidepressants
Photophysics and photochemistry

ABSTRACT

Phenothiazines derivatives are versatile compounds that are used in many fields, depending on the type and position of the substitution on the parent molecule. The photochemical, photophysical and electrochemical properties of several phenothiazine derivatives have been previously reported in detail. However, no reports have been presented for 2-aminophenothiazine (APH), a candidate that provides for the further chemical modification and the introduction of specific substituents. In this work, the photophysical and electrochemical properties of APH were measured in acetonitrile. The APH ground state absorption and fluorescence spectrum ($\Phi_f < 0.01$) are similar to the corresponding PH parent molecule. A mono-exponential decay fluorescence lifetime of 0.65 ns was determined for APH in acetonitrile. Characterization of the 355 nm nanosecond laser flash photolysis transient species reveals the presence of the triplet–triplet transient intermediate with a high intersystem crossing quantum yield ($\Phi_T = 0.72 \pm 0.07$), indicating that the APH main excited state deactivation channel is intersystem crossing. The oxidation potential of APH is lower than phenothiazine parent molecule (0.38 V vs. 0.69 V vs. Ag/AgCl(sat)). Altogether, these results show that APH has photochemical and photophysical properties similar to the phenothiazine parent molecule, but with the possibility of providing an amino functionality at 2-position for further chemical modification.

Published by Elsevier B.V.

1. Introduction

Phenothiazines (PH) and related derivatives are used in many applications including medicinal chemistry [1–3], polymer chemistry [3], sensors, and material science [4]. The usefulness of the PH derivatives is determined by the type and position of the substituent, because they strongly affect their redox, photophysical, and photochemical properties. The neuroleptic activity of the PH derivatives is greatly enhanced by substitution at the heterocyclic nitrogen with a propylamino chain [5]. Molecules bearing these properties are chlorpromazine, triflupromazine, and promethazine. Other molecules with similar pharmacological properties are derivatives having a propylperazine as the nitrogen side chain including thioridazine and trifluoperazine [5].

Tests showed that the substitution at the 2C-position apparently affects the tumor cell activity and the length of the aliphatic side chain at 10N contributes to the anti-tumor activity and the cytotoxicity of the drug [6]. 2-Trifluoromethyl phenothiazine, for instance, shows potent antitumor activity, whereas the corresponding chlorine derivative has a relative weak effect [7]. Biological relevant phenothiazine derivatives substituted at the 2C-position are also known to induce photosensitization of the skin after systemic use or topical applications [5]. Therefore, it is pertinent and relevant to search for new derivatives with less side effects and to acquire knowledge on their photophysical and photochemical properties that depend on the 2C-substitution.

We report herein the photophysical, photochemical, and electrochemical properties of 2-aminophenothiazine (APH) (Fig. 1) as alternative to other PH. The relevance of the present study is to provide new knowledge of this basic molecular structure, APH. The 2-amino group provides the possibility for further chemical modification through the amino group and also through the heterocyclic 10 position, serving as a precursor for other derivatives. In addition, quantum chemical calculations were performed to identify the electronic contributions of each atom to the corresponding electronic transitions.

2. Experimental/materials and methods

All chemicals were purchased from Sigma–Aldrich (USA). High quality spectrophotometric grade organic solvents were from well-

Abbreviations: APH, 2-aminophenothiazine; BP, benzophenone; βC, β-carotene; DFT, Density Functional Theory; Ea, anodic potential; MB, methylene blue; PH, phenothiazines; PDT, photodynamic therapy; POPOP, 1,4-bis(5-phenyloxazole-2-yl)benzene; SCE, saturated Calomel electrode; TCA, tricyclic antidepressants.

* Corresponding authors. Tel.: +1 787 850 9387; fax: +1 787 850 9422.
E-mail addresses: carmelo.garcia@upr.edu (C. García), rolando.oyola@upr.edu (R. Oyola).

1010-6030/$ – see front matter. Published by Elsevier B.V.
doi:10.1016/j.jphotochem.2008.02.028

known suppliers and used without further purification. All gases were purchased from Air Products (Humacao, PR).

2.1. Synthesis of APH

APH was synthesized using a modified method of the one reported by Nodiff and Hausman [4]. A vigorous stream of hydrogen chloride gas ($NaCl + H_2SO_4$) was passed into a suspension of 0.033 mol of stannous chloride dehydrate in 10 mL of glacial acetic acid until the suspension cleared. During this time, a solution of 0.0041 mol of 2-nitrophenothiazine, synthesized in our group, was dissolved in 5.00 mL of glacial acetic acid and the temperature of this solution was raised to 75 °C. After the suspension is added, the temperature mixture increased to 110 °C and the solution changed from red to black. Few seconds later, a white solid began to form and the solution color turned brown. The reaction was completed in 15 min. The reaction mixture was filtered and the filtrate was poured onto crushed ice. The resulting precipitate was recrystallized from a dichloromethane/carbon tetrachloride mixture to give 0.563 g (64%) of the solid. Mass spectrum: 214.04 (100), 182.07 (70), 154.06 (15), 107 (15). Infrared: 3404 and 3322 cm^{-1}, primary and heterocyclic secondary amine, respectively.

2.2. Synthesis of 2-nitrophenothiazine

A of 1:1 mixture of 2-bromo-2′-formamido-4′-nitrodiphenyl sulfide and K_2CO_3 (0.040 mol), 0.0017 mol of $CuCO_3$, and 140 mL of *p*-xylene were stirred and heated until reflux [8]. A water separator was attached to the reflux condenser to collect the few drops of water generated by this reaction. The reaction was followed by thin layer chromatography (Silica gel, 90% hexane/10% ethyl acetate). Once the limiting reagent reacted, the mixture was allowed to stand at room temperature, producing a brown precipitate that was filtrated under vacuum and evaporating the solvent. The residue was added to a sodium hydroxide solution and the mixture was refluxed for 2 h, then it was filtrated and the black solid was recrystallized from toluene. A violet precipitate, 2-nitrophenothiazine, was obtained and characterized using NMR, MS, and FTIR techniques: ^{1}H: 9.01 (s, 1H), 7.60–7.59 (d,d 1H, J = 2.40 Hz, J = 8.47 Hz), 7.46–7.45 (d, 1H, J = 2.41 Hz), 7.18–7.16 (d, 1H, J = 8.47 Hz), 7.10–7.06 (d,d,d, 1H, J = 1.36 Hz, J = 7.64 Hz, J = 15.28 Hz), 6.99–6.94 (d,d, 1H, J = 1.20 Hz, J = 7.67 Hz), 6.87-6.83 (d,d,d 1H, J = 1.10, J = 7.53 Hz, J = 15.01 Hz), 6.70–6.68 (d,d 1H, J = 1.00 Hz, J = 7.91 Hz). ^{13}C: 108.0, 115.1, 115.2, 116.9, 123.2, 126.8, 127.0, 128.8, 140.6, 143.1, 147.5; MS: 244 (100%) molecular ion (base peak), 198 (75), 171 (11), 154 (18); IR: (N—H) 3341, (-NO_2) 1504 and 1324.

2.3. Absorption and emission spectroscopy

Absorption spectra were taken with a HP 8453 UV–vis photodiode array spectrophotometer. Luminescence was measured with a Spex Fluorolog Tau 3.11 spectrofluorimeter with fluorescence lifetimes capabilities (Spex Industries, NJ). The fluorescence quantum yield (Φ_f) was obtained relative to quinine sulfate (Φ_f = 0.55) [9]. The excitation wavelength was 340 nm, reference and samples were optically matched (A < 0.1) and the monochromator slits were both set at 2.0 nm. Corrections were made for differences in the instrument sensitivity as a function of wavelength and for differences in refractive index. The frequency-response of the sample, in which the phase-shift and modulation of the sample are measured as a function of frequency, was obtained against a scatter solution or POPOP (τ_f = 1.35 ns) for the determination of the fluorescence lifetime [9].

2.4. Nanosecond transient absorption spectroscopy

The nanosecond spectrokinetic system has been described elsewhere [10–12]. Briefly, the 355 nm harmonic of a Nd/YAG Continuum Surelite II Laser was used for sample excitation with the following standard conditions: pulse duration = 5 ns, repetition rate = 10 Hz, laser irradiation area = 0.30 cm^2, and maximum fluence = 2.8×10^{-5} mmol/cm^2). The laser fluence was measured using the benzophenone triplet–triplet absorption at 520 nm in acetonitrile. Transient absorption spectra were taken using a $1 \times 1 \times 4$ cm flow-through cell connected to a relatively larger reservoir to minimize photodegradation. The kinetics at one wavelength were determined using static samples for which no more than ten laser pulses were averaged to avoid sample degradation. Transient species were monitored at a right angle to the laser beam using a 300 W Xenon arc lamp (Oriel Corp.), a monochromator (Model 300, Acton Research) and a Hamamatsu R928 five-stage dynode wired photomultiplier tube, and 400 MHz bandwidth oscilloscope Model 9310 (Lecroy Corp.). All the spectrokinetic system was controlled with an in house software application developed under LabView 8.0 (National Instruments, Austin, TX).

2.4.1. Determination of triplet absorption coefficient (ε_T)

Triplet absorption coefficients were measured in solution using the energy transfer method [13]. Briefly, a solution of APH in CH_3CN was excited at 355 nm in the absence and in the presence of 73 μM methylene blue cation (MB). The ε_T^{APH} value for $^3APH^*$ was determined according to $\varepsilon_T^{APH} = (\varepsilon_T^{MB} \Delta A_T^{APH})/\Delta A_T^{MB}$ were ΔA_T^{APH} is the triplet absorbance of APH in the absence of MB, ΔA_T^{MB} is the MB triplet absorbance following energy transfer from $^3APH^*$ donor, and $\varepsilon_T^{MB} = 14,400\,(M\,cm)^{-1}$ for $^3MB^*$ at 420 nm [15].

2.4.2. Quantum yields of triplet formation (Φ_T)

This value was obtained by the comparative actinometry method using benzophenone triplet ($^3BP^*$) in acetonitrile as reference ($\Phi_T^{BP} = 1.00$, $\varepsilon_T^{BP} = 6500\,M^{-1}\,cm^{-1}$ at 520 nm) [13]. Optically matched samples of BP and APH were irradiated with the 355 nm laser line in the nitrogen-saturated solvent. The triplet state absorbance of BP at 520 nm (ΔA_T^{MB}) and of APH (ΔA_T^{APH}) at 480 nm were measured at different laser intensities. A plot of ΔA_T of BP and APH as a function of laser fluence was then used to calculate the quantum yield of triplet formation of APH (Φ_T^{APH}) according to $\Phi_T^{APH} = (\Phi_T^{BP} \varepsilon_T^{BP} \alpha_T^{APH})/(\varepsilon_T^{APH} \alpha_T^{BP})$ were ε_T is the triplet molar absorption coefficient of BP or APH, and α_T is the triplet aborbance per laser fluence (mmol/cm^2) for BP or APH, respectively.

2.5. Electrochemical measurements

APH (3.0 mM) solutions for cyclic voltammetry (CV) measurements were prepared in acetonitrile (dried over molecular sieves) in the presence of 0.1 M supporting electrolyte tetra-butyl ammonium per-chlorate (re-crystallized from ethyl acetate and dried for 1 h at 120 °C). All solutions were degassed before use to avoid reactions with oxygen. The voltammograms were recorded in an EC Epsilon Electrochemical Analyzer (BAS Inc., USA). The three electrode system consisted of the glassy carbon (GC) working electrode and a reference silver–silver chloride(sat) [Ag/AgCl(sat)] electrode and platinum counter electrode. The reference electrode formal potential was corroborated against ferrocene as internal standard (0.449 V vs. SCE in acetonitrile) [14,15]. Before every scan, the working electrode was polished carefully with diamond paste, rinsed with deionized water, placed in the sonic bath for two minutes in a methanol/acetone mixture and rinsed once again in deionized water. All experiments were carried out at room temperature.

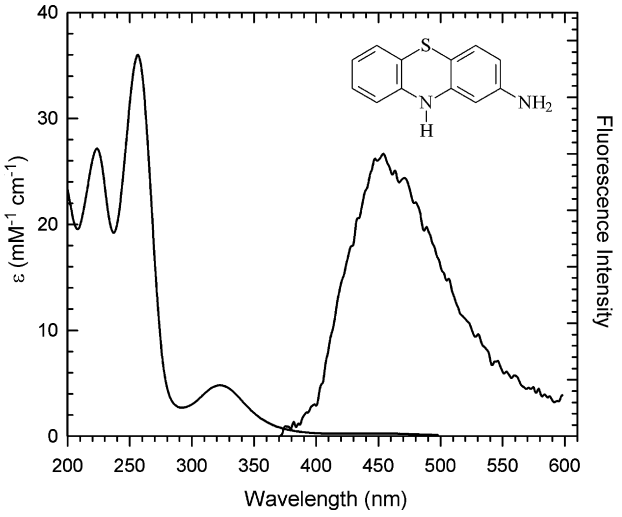

Fig. 1. Absorption (left) and emission (right) spectrum of APH in acetonitrile. *Insert*: APH structure.

2.6. Theoretical calculations

Geometry pre-optimization using a combination of molecular mechanics (MM+), molecular dynamics and quantum mechanical calculations for closed shells (PM3/RHF/CI) and open shells (PM3/UHF) were done with HyperChem 8.0 (HyperCube Inc., Florida). The half-electron method was used for the S1-excited state (PM3/HE). At the semiempirical level, the optimizations were done with the Polak-Ribiere conjugated gradient protocol (1×10^{-5} convergence limit and 0.001 kcal/Å mol RMS-limit) [16]. Full optimization and calculations of all molecular parameters were obtained with DFT (B3LYP/6-31G(d)) using Gaussian 03 at the BobSCEd cluster (Earlham College Cluster Computing Group; Richmond, IN). The spectroscopic data was obtained with CI-single point calculations using three occupied and three virtual orbitals.

3. Results and discussion

3.1. Ground state properties

The absorption spectrum of APH in acetonitrile shows three main peaks at 224, 256, and 322 nm with corresponding molar absorptions extinction coefficients of $(2.48 \pm 0.01) \times 10^4$, $(3.59 \pm 0.01) \times 10^4$ and $(4.80 \pm 0.01) \times 10^3$ M^{-1} cm^{-1} (Fig. 1).

The high extinction coefficients of the short wavelength transitions are indicative of their π–π^* character. The peak at 322 nm was assigned to an n–π^* transition, as previously reported for the phenothiazine derivatives [11].

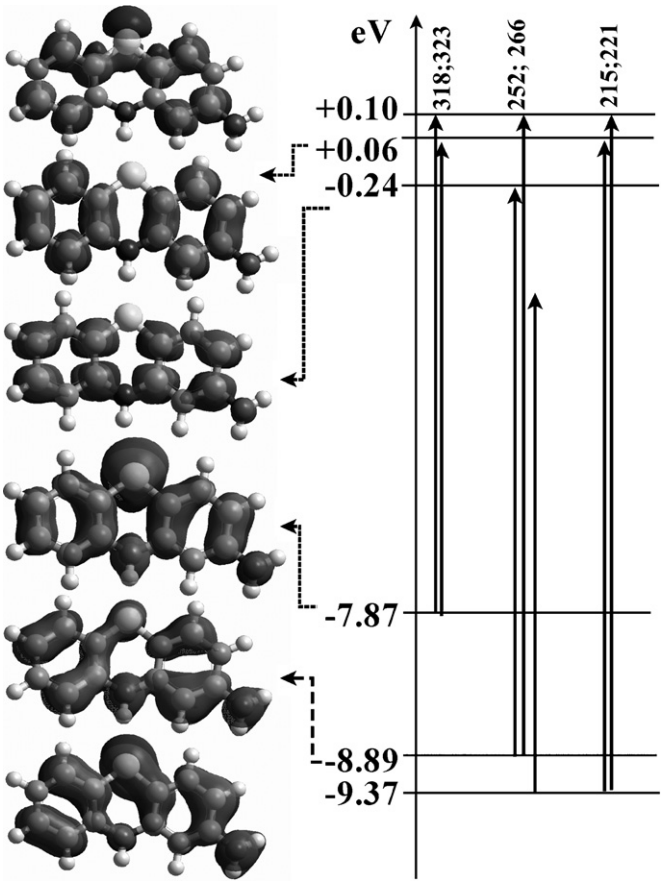

Fig. 2. Electronic transitions and corresponding orbitals of APH.

To better understand the contribution of the atomic orbitals to these electronic transitions, quantum theoretical calculations were performed. The semi-empirical calculations predict at least two electronic transitions for each one of the observed bands (Table 1), in excellent agreement with the experimental data. Fig. 2 shows the molecular orbitals involved in these transitions and corroborate the participation of the amine *n*-electrons in the 322 nm transition.

In addition, the ground state of APH is not planar, showing a dihedral angle of 153°. This non-planarity is common to all phenothiazine derivatives, and is often affected by substitution at 2C and 3C positions [10,17,18]. It is apparent that the 2-amino substi-

Table 1
Theoretical parameters for phenothiazine parent compound and APH

Substance	State	ΔH (kcal/mol)	μ (D)	Torsion angle (°)	λ (nm[f])[a]
Phenothiazine	S0	59.7	2.3	153	208[0.08], 234[0.02] 253[0.32], 262[108] 323[0.11], 326[0.15]
	S1	113.3	3.6	180	–
	T1	96.3	3.4	174	344[0.01], 517[0.12]
APH	S0	57.2	2.4	153	215[0.47], 221[0.08] 252[0.12], 266[1.02] 318[0.14], 323[0.27]
	S1	117.4	2.4	180	–
	T1	93.8	3.9	172	346[0.16], 498[0.08]

[a] Oscillator strength.

Table 2
Photophysical and electrochemical properties of APH in acetonitrile

Property	Value
ε_{320}	$(4.80 \pm 0.01) \times 10^3$ (M cm)$^{-1}$
Φ_f	<0.01
τ_f	0.65 ns
k_f	1.5×10^7 s^{-1}
k_{ic}	3.9×10^8 s^{-1}
ε_T	$(1.4 \pm 0.2) \times 10^4$ (M cm)$^{-1}$
Φ_T	0.72 ± 0.07
k_{isc}	1.1×10^9 s^{-1}
k_0	$(8.1 \pm 0.9) \times 10^4$ s^{-1}
k_{sq}	$(5.9 \pm 0.2) \times 10^8$ M^{-1} s^{-1}
E_{ox} vs. Ag/AgCl	0.38 V

tution, in this case, does not change the ground state conformation of APH relative to PH.

3.2. Excited singlet state properties

APH shows a broad fluorescence emission spectrum with maximum at 450 nm (Fig. 1). A Φ_f value lower than 0.01 was determined against quinine sulfate. This low Φ_f value is common to PH derivatives [10]. A singlet energy of 75 kcal/mol was calculated from the crossing point of the excitation and emission spectra. This value is similar to phenothiazine parent compound (77 kcal/mol) [19]. A singlet fluorescence lifetime 0.65 ± 0.08 ns was measured for air-saturated acetonitrile APH solution (Table 2).

This fluorescence lifetime is similar to that of the corresponding phenothiazine parent molecule in acetonitrile ($\tau_f = 0.84$ ns) [20]. These results show that, for APH, emission is not a major deactivation pathway, similar to other phenothiazine derivatives [10]. A plausible major deactivation mechanism should then be intersystem crossing and to verify this, laser flash photolysis studies were performed.

3.3. Nanosecond laser flash photolysis

3.3.1. Transient absorption spectra

The 355 nm laser induced transient absorption spectrum of a nitrogen-saturated acetonitrile APH solution is shown in Fig. 3. Two absorption bands with maxima at 380 and around 480–500 nm are observed.

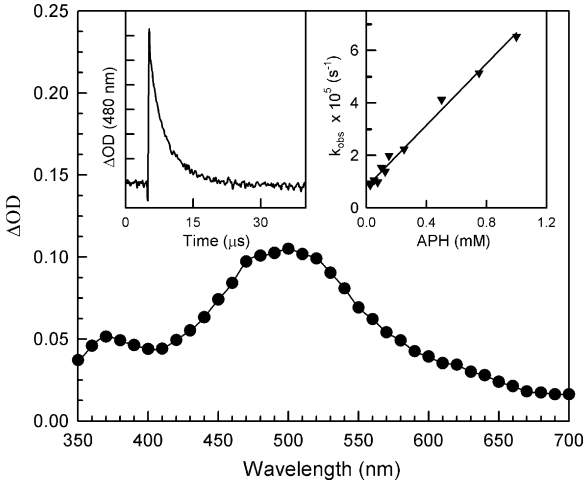

Fig. 3. Flash photolysis transient absorption spectrum of 0.25 mM APH recorded in nitrogen-saturated solution at 500 ns after the laser pulse. Inset: decay time profile at 480 nm (top left) and the observed ^{3}APH* decay first order rate constant (k_{obs}) at 480 nm against APH ground state concentration (top right).

The kinetic decays at both wavelengths are similar and are best described by first order fits with lifetime of 3.5 ± 0.3 μs. To characterize the short-lived intermediates, the transient absorption spectra were measured in air-saturated acetonitrile solution maintaining all other experimental parameters constant. Under these conditions, the dissolved oxygen greatly enhances the decay rate constant ($1/k \approx 35$ ns). Based on the effect of oxygen upon the rate constant, the transient species is assigned to the triplet state of APH (^{3}APH*). To verify this assignment, a flash photolysis transient absorption spectrum was recorded for a solution containing 0.80 mM APH and 40 μM β-carotene (βC). βC is commonly used to evaluate the presence of triplets due to its low triplet energy ($E_T = 21$ kcal/mol) [13]. The results showed that, indeed, βC efficiently quenches the ^{3}APH*, as demonstrated by the formation of its characteristic ^{3}βC* absorption band at 510 nm immediately after the laser pulse.

Theoretical calculations were performed to better understand the APH triplet excited state conformation. DFT calculations predict only one stable conformation for the ^{3}APH* (Table 1). It has a torsion angle of 172°, which makes it more planar than the ground state. This is also consistent with other PH derivatives, which also have more planar excited states [11]. The PM3 calculations predict triplet–triplet bands at 346 and 498 nm, all with relative low molar absorption coefficient. The agreement with the experimental values is good, although, these theoretical excited state calculations suffer from large spin contamination.

The effect of high intensity laser pulses in the transient absorption spectra was evaluated using fluences higher than 10 mJ/pulse in sodium dodecyl sulfate aqueous solution. At these higher laser intensities, new bands in the transient absorption spectra were observed. These bands were attributed to a laser-induced photoionization process due to the presence of the solvated electron absorption in the visible region (broad band between 400 and 750 nm) under nitrogen-saturated solution, and secondary radicals with absorption maximum at 600 nm. Therefore, in order to minimized nonlinear photon processes, all other experiments were performed at low laser intensity ($E < 5$ mJ/pulse).

The effect of the APH ground state concentration on the ^{3}APH* decay rate constant in acetonitrile was studied using the Stern–Volmer relationship. The observed first-order rate constants (k_{obs}) obtained from the decay of ^{3}APH* are plotted as a function of the ground state concentration. This relationship should follow a straight line according to the following equation: $k_{obs} = k_0 + k_{sq}$ [APH], where k_0 and k_{sq} represent the decay rate of ^{3}APH* at the infinitely diluted concentration and the self-quenching rate constant, respectively. The k_{sq} determined was $(5.9 \pm 0.2) \times 10^8$ M^{-1} s^{-1} (Fig. 3). The magnitude of k_{sq} for ^{3}APH* is similar to other PH derivatives [10,15,21]. The k_0 determined was $(8.1 \pm 0.9) \times 10^4$ s^{-1} ($\tau_0 = 1/k_0 \approx 12.5$ μs), which is also similar to the value of the PH parent molecule.

3.3.2. Characterization of the excited triplet state

To determine the APH intersystem crossing quantum yield (Φ_T), its triplet molar absorption coefficient is required. Fig. 4A shows the transient absorption spectrum of a 0.38 mM nitrogen-saturated acetonitrile solution of APH containing 73 μM MB.

Under these conditions, more than 90% of the laser light is absorbed by APH. The spectrum at 100 ns after the laser pulse shows bands with maxima at 420 and 510 nm. The spectra at subsequent times show an intensity decrease and a red shift of the 510 nm band with a concomitant increase of the absorption at 420 nm. The spectrum at 8 μs, when ^{3}APH* has decayed completely, shows a maximum at 420 and 525 nm. This spectrum is in excellent agreement with the photosensitized triplet–triplet absorption spectrum of MB by benzophenone in acetonitrile reported by Jockusch et al.

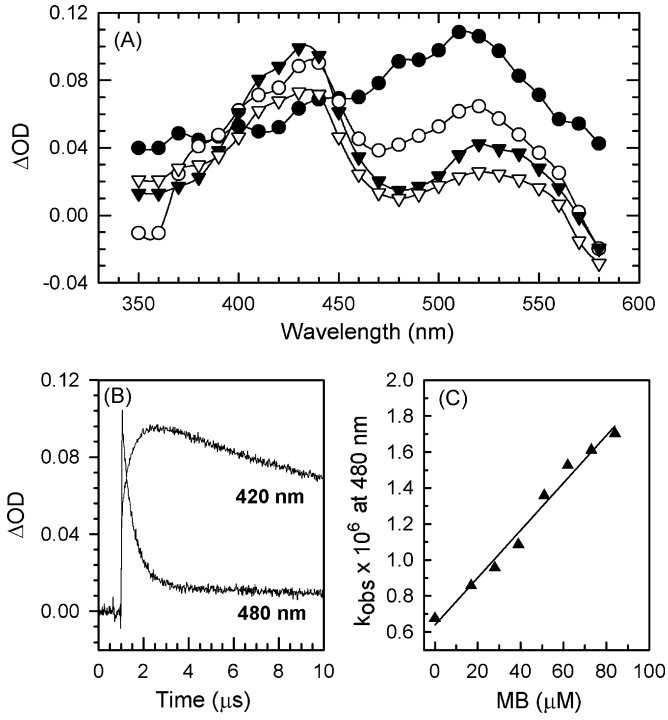

Fig. 4. (A) Flash photolysis transient absorption spectra of a nitrogen-saturated acetonitrile solution of 0.38 mM APH and 73 μM MB at (●) 100 ns, (○) 600 ns, (▼) 1.7 μs, and (▽) 8 μs after the laser pulse. (B) Time profile decays response at 420 nm and 480 nm, and (C) Stern–Volmer analysis for the ^{3}APH* + MB energy transfer processes.

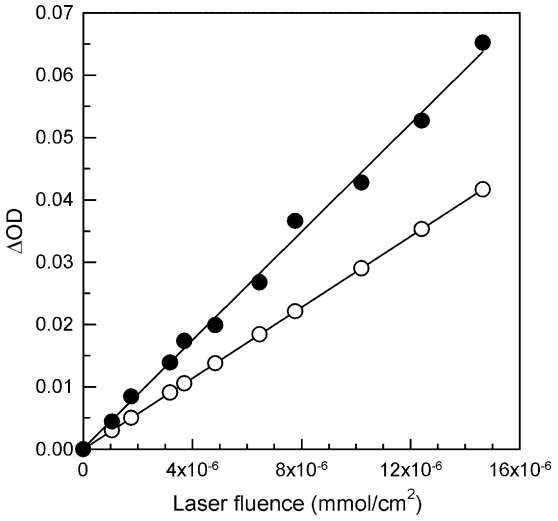

Fig. 5. Power dependance of the triplet–triplet absorption of (●) APH and (○) BP.

[22]. In addition, the decay lifetime of 0.63 μs at 480 nm matches very well with the kinetic growth at 420 nm (Fig. 4B). Moreover, the photosensitized ^{3}MB* decays with a lifetime of 31 μs, is also in good agreement with the reported value of 35 μs [22]. Based on all these results, we propose that the 355 nm laser excitation of APH results in an energy transfer process from ^{3}APH* to MB, producing ^{3}MB*. The quenching rate constant for this process (k_q) was determined by measuring the decay rate constant at 480 nm (k_{obs}) as a function of the MB concentration and using the Stern–Volmer analysis ($k_{obs} = k_0 + k_q$ [MB]). At this wavelength, MB shows almost no absorption, while ^{3}APH* is close to its maximum. A diffusion controlled quenching rate constant of $(1.31 \pm 0.07) \times 10^{10}$ M^{-1} s^{-1} was determined (Fig. 4C). This rate constant is 1.6 times higher than that for the couple of ^{3}BP* and MB ($k_q = 8.5 \times 10^9$ M^{-1} s^{-1}) [22]. Because an energy transfer processes occurs, the APH triplet molar absorption coefficient was determined from the kinetic growth of ^{3}MB* and the ^{3}APH* decay as described in Section 2.4.1. The ε_T for ^{3}APH* was determined to be $(1.4 \pm 0.2) \times 10^4$ M^{-1} cm^{-1}.

The Φ_T was determined using the comparative method as described in 2.4.2. Fig. 5 shows the ^{3}APH* and ^{3}BP* transient absorbance at the end of the laser pulse as a function of laser fluence.

From the slopes of each plot, the Φ_T^{APH} in acetonitrile was determined to be 0.72 ± 0.07. This value is in agreement with the observed low fluorescence quantum yield. Therefore, the main deactivation channel for the APH excited singlet state is, in fact, intersystem crossing. These results are consistent with the reported high Φ_T values of other PH derivatives [23].

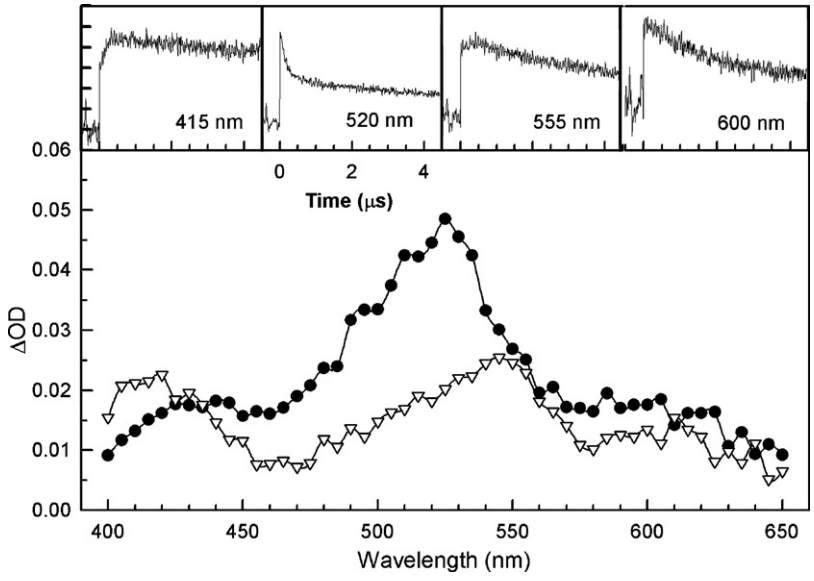

Fig. 6. Lower panel: transient absorption spectra of a nitrogen-saturated solution containing 35 mM BP and 0.10 mM APH at (●) 50 ns and (▽) 1.7 μs after the laser pulse. Top from left to right: transient absorption decay profiles at 415, 520, 555, and 600 nm.

It is well documented that amines quench the ketones triplet excited state [22]. The quenching mechanism may involve either an energy transfer, electron transfer, or hydrogen transfer mechanism. Whatever process takes place, depends on the amine–ketone pair and on the solvent [22]. Since APH has an amino group, it might be able to quench the BP triplet state. Therefore, we measured the transient absorption spectra of BP in the presence of APH, under the conditions that most of the 355 nm light is absorbed by BP. Fig. 6 shows the transient absorption spectra of BP in the presence of APH in nitrogen-saturated acetonitrile solution.

At 50 ns after the laser pulse it is clearly seen the $^3BP^*$ absorption band with maximum at 520 nm, and two smaller broad bands with maxima at 430 and 600 nm, respectively. The transient absorption spectrum at 1.7 μs after the laser pulse consists of three bands with maxima at 420, 545, and 600 nm. The transient absorption decay profiles at different wavelengths are also shown in Fig. 6. It is clearly seen that the signal at 415 and 555 nm grows with time. The 415 and 555 nm bands are attributed to an aminyl radical, centered at the 10-position heterocyclic nitrogen, and BP ketyl radical, respectively, indicative of a hydrogen transfer processes. The hydrogen atom at 10 position (heterocyclic nitrogen) has a lower pK_a than that of the amine group. Thus, it is expected that the aminyl radical correspond to the heterocyclic nitrogen.

3.4. Electrochemical studies

The cyclic voltammogram of APH (3 mM)/0.1 M TBAP in acetonitrile is depicted in Fig. 7. Upon scanning towards positive potentials, three well defined oxidation waves were observed between 0.34 and 1.0 V vs. Ag/AgCl(sat).

More negative the ability to donate electrons increases with decreasing positive anodic potential (Ea), therefore, based on the potential of the first oxidation, APH (Ea(APH) = 0.380 V vs. Ag/AgCl(sat)) has a relative higher oxidation ability than the parent hydrocarbon phenothiazine in acetonitrile (Ea(PH) = 0.697 V vs. Ag/AgCl(sat)) measured under identical conditions. Comparison with other 2-PH was not possible since to our best knowledge, the oxidation potentials for phenothiazine derivatives substituted at position 2 have not been reported in acetonitrile. Therefore, we proceeded to measure the oxidation potentials in acetonitrile of a series of 2-substituted PH derivatives synthesized in our group. The following trend of decreasing oxidation ability was obtained: APH (0.380 V) > phenothiazine (0.697 V) > 2-chlorphenothiazine (0.730 V) > 2-nitrophenothiazine (0.902 V). These results indicate that the stability of the first oxidation product of a given phenothiazine derivative depends on the effect of the *ortho*, *para* or *meta* directing capacity that the substituents in the tricyclic moiety have on the oxidation potentials of a specific phenothiazine derivative. This in turn is related to the Hammett's substituent constants, which associate the reaction rates with the electron-withdrawing ability of the substituent [24]. Consequently, the stability of the first oxidation product of the phenothiazines depends on the electron-withdrawing ability of the substituent. Some authors have stated that the nitrogen atom in the phenothiazine cation radical is a center of the strongest Lewis acidity and that this property probably leads to strong coordinating interactions of the solvent molecules [25].

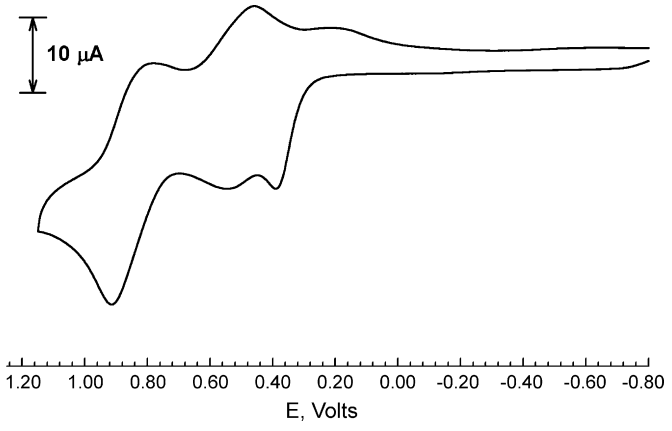

Fig. 7. Cyclic voltammogram of 3.0 mM APH on a glassy carbon electrode in acetonitrile containing 0.1 M TBAP at a scan rate of 100 mV/s.

Further electrochemical characterization of the voltammogram of APH shows that the following oxidations present peak distortions due to the adsorption of the oxidized products on the electrode surface. This was corroborated with scan rate variations and multiple cycles. Therefore, further irreversible oxidations of APH can be attributed to short-lived intermediates that react, after oxidation of the cation radical. A similar electrochemical behavior has been observed with the oxidized phenothizine parent compound, which after oxidizing to the cation radical undergoes deprotonation, dimerization, and/or further oxidation [26]. Furthermore, the electrochemical irreversibility of some phenothiazine derivatives has been attributed to chemical reaction with trace water or with the solvent, acetonitrile [27]. It has also been established that the phenothiazine cation radical in aprotic media is in equilibrium with the protonated and deprotonated radicals and the oxidation reversibility increases in acidic conditions [28]. Therefore, the stability of the oxidation product of a given phenothiazine derivative depends on the solution conditions (i.e. solvent, pH), leading either to disproportionation to form a radical dication and the original phenothiazine or to an additional electrochemical oxidation to form a dication radical.

Phenothiazines could participate in photoinduced electron transfer processes. The driving force for photoinduced electron transfer (ΔG_{et}) can be estimated according to Rehm and Weller [29],

$$\Delta G_{et} = 23.06 \left[E_{ox}(D) - E_{red}(A) - \left(\frac{e^2}{\varepsilon a} \right) \right] - E_{00} \quad (1)$$

where ΔG_{et} is the free energy for electron transfer in kcal/mol, $E_{ox}(D)$ is the oxidation potential of the donor (0.38 V for APH), $E_{red}(A)$ is the reduction potential of the acceptor, E_{00} (60.4 kcal/mol) [19] is the excitation energy of the donor and the ($e^2/\varepsilon a$) is the solvent dependent Coulomb term, which is frequently neglected in polar solvents such as acetonitrile (0.5 eV). It is interesting to note that for APH as donor and any acceptor with E_{red} more negative than approximately −2.20 V leads to an exergonic electron transfer processes in the presence of ^{3}APH. On the other hand, the photo oxidation of APH excited singlet state will be exergonic with any electron acceptor with E_{red} more negative than −2.87 V.

4. Conclusions

The photochemical and photophysical properties of 2-aminophenothiazine were determined in acetonitrile. A low fluorescence emission yield is correlated to a high triplet quantum yield formation. The lower oxidation potential for APH relative to phenothiazine parent compound could increase the efficiency of electron transfer processes. A property that can be exploited in the area of material science. A Φ_T of 0.72 ± 0.07 indicates that this molecule can be a potential photosensitizer for light inactivation of viruses and bacteria or in PDT. Finally, the amino substitution will serve as a precursor for the synthesis of other phenothiazine derivatives with substitution at two position.

Acknowledgments

This work has been supported in part by NIH-S06GM08216 and NSF-SBE0123645 grants to the University of Puerto Rico-Humacao. C. García thanks to the Earlham College Cluster Computing Group for the computer access to run the theoretical calculations.

References

[1] M. Wainwright, H. Mohr, W.H. Walker, J. Photochem. Photobiol. B 86 (2007) 45–58.
[2] H. Lacasse, M.M. Perreault, D.R. Williamson, Ann. Pharmacother. 40 (2006) 1966–1973.
[3] M. Barra, R.W. Redmond, M.T. Allen, G.S. Calabrese, R. Sinta, J.C. Scaiano, Macromolecules 24 (1991) 4972–4977.
[4] E.A. Nodiff, M. Hausman, J. Org. Chem. 29 (1964) 2453–2455.
[5] S.C. Mitchell, Curr. Drug Targets 7 (2006) 1181–1189.
[6] T. Kurihara, N. Motohashi, H. Sakagami, J. Molnar, Anticancer Res. 19 (1999) 4081–4083.
[7] S. Nagy, G. Argyelan, J. Molnar, M. Kawase, N. Motohashi, Anticancer Res. 16 (1996) 1915–1918.
[8] G. Eregowda, H. Kalpana, R. Hedge, K. Thimmaiah, Indian J. Chem. 39B (2000) 243–259.
[9] J.R. Lakowicz, Principles of Fluorescence Spectroscopy, 3rd ed., Springer Science, New York, USA, 2006.
[10] C. Garcia, R. Oyola, L.E. Pinero, R. Arce, J. Silva, V. Sanchez, J. Phys. Chem. A 109 (2005) 3360–3371.
[11] C. Garcia, R. Oyola, L.E. Pinero, N. Cruz, F. Alejandro, R. Arce, I. Nieves, J. Phys. Chem. B 106 (2002) 9794–9801.
[12] R. Arce, C. Garcia, R. Oyola, L.E. Pinero, I. Nieves, N. Cruz, J. Photochem. Photobiol. A: Chem. 154 (2003) 245–257.
[13] R.V. Bensasson, E.J. Land, T.G. Truscott, Excited States and Free Radicals in Biology and Medicine: Contributions from Flash Photolysis and Pulse Radiolysis, Oxford University Press, New York, USA, 1993.
[14] R.L. Konkers, M.S. Workentin, Chem. Eur. J. 7 (2001) 4012–4019.
[15] Y. Gao, J. Chen, X. Zhuang, J. Wang, Y. Pan, L. Zhang, S. Yu, Chem. Phys. 334 (2007) 224–231.
[16] A. Jouyban, B.H. Yousefi, Comput. Biol. Chem. 27 (2003) 297–303.
[17] G. Viola, F. Dall'Acqua, Curr. Drug Targets 7 (2006) 1135–1154.
[18] W. Caetano, L.R. Barbosa, R. Itri, M. Tabak, J. Colloid Interface Sci. 260 (2003) 414–422.
[19] M. Montalti, A. Credi, L. Prodi, T.M. Gandolfi, Handbook of Photochemistry, 3rd ed., CRC Press Taylor & Francis Group, 2006.
[20] G. Pohlers, J.C. Scaiano, R. Sinta, R. Brainard, D. Pai, Chem. Mater. 9 (1997) 1353–1361.
[21] T. Rodrigues, C.G. dos Santos, A. Riposati, L.R. Barbosa, M.P. Di, R. Itri, M.S. Baptista, O.R. Nascimento, I.L. Nantes, J. Phys. Chem. B 110 (2006) 12257–12265.
[22] S. Jockusch, H.J. Timpe, W. Schnabel, N.J. Turro, J. Phys. Chem. A 101 (1997) 440–445.
[23] I. Carmichael, G.L. Hug, J. Phys. Chem. Ref. Data 15 (1986) 1–250.
[24] P.H. Sackett, J.S. Mayausky, T. Smith, S. Kalus, R.L. McCreery, J. Med. Chem. 24 (1981) 1342–1347.
[25] B. Paduszek, M.K. Kalinowski, Electroquimica Acta 28 (1983) 639–642.
[26] J.F. Evans, J.R. Lenhard, H.N. Blount, J. Org. Chem. 42 (1977) 983–988.
[27] R.Y. Lai, E.F. Fabrizio, L. Lu, S.A. Jenekhe, A.J. Bard, J. Am. Chem. Soc. 123 (2001) 9112–9118.
[28] S. Nomura, Y. Morishima, T. Koremoto, M. Kamachi, J. Polym. Sci: Part A: Polym. Chem. 32 (1994) 1703–1710.
[29] D. Rehm, A. Weller, Ber: Bunsen-Ges. Phys. Chem. 73 (1969) 834–839.